Biodistribution of therapeutic small interfering rnas delivered with lipid-substituted polyethylenimine-based delivery systems

Morales, Luis C.; Rajendran, Amarnath; Ansari, Aysha; KC, Remant; Nasrullah, Mohammad; Kiti, Kitipong; Yotsomnuk, Panadda; Kulka, Marianna; Meenakshi Sundaram, Daniel Nisakar; Uludağ, Hasan

Publisher's version / Version de l'éditeur:
https://doi.org/10.1021/acs.molpharmaceut.3c01077
Molecular Pharmaceutics, 21, 3, pp. 1436-1449, 2024-01-30

Biodistribution of Therapeutic Small Interfering RNAs Delivered with Lipid-Substituted Polyethylenimine-Based Delivery Systems

Morales Burbano, Luis Carlos; Rajendran, Amarnath; Ansari, Aysha; KC, Remant; Nasrullah, Mohammad; Kiti, Kitipong; Yotsomnuk, Panadda; Kulka, Marianna; Meenakshi Sundaram, Daniel; Uludag, Hasan

[1] Department of Chemical and Materials Engineering, Faculty of Engineering, University of Alberta, Edmonton, AB, Canada

[2] Faculty of Pharmacy and Pharmaceutical Sciences, University of Alberta, Edmonton, AB, Canada

[3] School of Science, Mae Fah Luang University, Thailand.

[4] Department of Chemical Engineering, Thammasat School of Engineering, Thailand

[5] Department of Biomedical Engineering, Faculty of Medicine and Dentistry, University of Alberta, Edmonton, AB, Canada

Correspondence: Hasan Uludağ, e-mail: huludag@ualberta.ca

ABSTRACT

Small interfering RNAs (siRNAs) have emerged as powerful tool to manipulate gene expression *in vitro*. However, their potential therapeutic application encounters significant challenges, such as degradation *in vivo,* limited cellular uptake and restricted biodistribution, amongst others. This study evaluates the siRNA delivery efficiency of three different lipid-substituted polyethylenimine (PEI) based carriers, named Leu-Fect A, B and C, to different organs *in vivo*, including xenograft tumors, when injected into the bloodstream of mice. The siRNA analysis was undertaken by stem-Loop RT-PCR, followed by qPCR or digital droplet PCR. Formulating siRNAs with Leu-Fect series of carriers generated nanoparticles that effectively delivered the siRNAs into K652 and MV4-11 cells, both models of leukemia. The Leu-Fect carriers were able to successfully deliver BCR-Abl and FLT3 siRNAs into leukemia xenograft tumors in mice. All three carriers demonstrated significantly enhanced siRNA delivery into organs other than liver, including the xenograft tumors. Preferential biodistribution of siRNAs was observed in the lungs and spleen. Amongst the delivery systems, Leu-Fect A exhibited the highest biodistribution into organs. In conclusion, lipid-substituted PEI-based delivery systems offer improvements in addressing pharmacokinetic challenges associated with siRNA-based therapies, thus opening avenues for their potential translation into clinical practice.

INTRODUCTION

During the last two decades, there has been a growing interest in therapeutic nucleic acids and their potential to become a central paradigm in the treatment or prevention of common diseases [1]. Advances in gene sequencing and gene therapy have allowed scientist to identify causative gene defects, or potential immunogens in the case of vaccines, and quickly develop therapies based on nucleic acids that is tailored for particular diseases [2]. The most well-known example of such an approach is the recent COVID-19 pandemic, where exogenous mRNA was used to instruct human cells to produce a immunogenic viral protein, and therefore create long-term immunity in the vaccine recipients [3]. Alternatively, nucleic acids can be also used to reduce the production of a harmful protein when required. For instance, Patisiran (Ompattro®, Alnylam) is based on small interfering RNA (siRNA), designed to decrease the production of transthyretin (TTR) in patients suffering from hereditary variant TTR amyloidosis (ATTRv), a rare autosomal dominant disorder where misfolded mutated TTR accumulates in various tissues throughout the body, causing neuropathy and/or cardiomyopathy in said patients [4]. Therapeutic nucleic acids are also being explored for more prevalent conditions, as in the case of siRNA drug Zilebesiran (Roche and Alnylam), which is designed to decrease the liver production of angiotensinogen, a key player in the pathophysiology of high blood pressure [5]. Zilebesiran was effective in decreasing serum angiotensinogen levels and 24h ambulatory blood pressure in patients enrolled in a Phase 1 study [5] and, at the time of writing of this manuscript, is being tested in 2 separate Phase 2 studies.

One of the main challenges facing therapeutic nucleic acids when attempting to transition into the clinic is that nucleic acids display physical characteristics that do not favor biodistribution and cellular uptake, meaning that their negative charge, large molecular mass and low hydrophobicity, make cell membranes almost impermeable to them. Time spent in circulation poses a major treat

to efficacy since most of the molecules will not reach their destination with the same ease as small molecules and they could be degraded by endogenous enzymes during this time. For this reason, delivery vehicles have been designed to facilitate *in vitro* delivery and *in vivo* biodistribution [6]. While viral carriers provide high transfection efficiency, their efficacy is quickly overcome by the host's immune system. Moreover, using viruses as delivery vehicles have higher rates of side effects and the amount of therapeutic nucleic acids that can be packed into a virus (vector capacity) is limited [7,8]. On the other hand, non-viral carriers, including nanoparticles constructed from lipids, inorganic molecules (such as gold) and cationic polymers (such as chitosan and polyethylenimine, PEI) are safer with low immunogenicity and mutagenic potential, and offer manufacturing advantages especially at the scale-up step [9]. The advantages and disadvantages of viral vectors vs. non-viral delivery vehicles are summarized in Table 1.

Viral Vectors	**Non-viral vectors**
High delivery efficacy	Low delivery efficacy
Tissue/cell tropism	Challenging targeting
Immunogenic	Low immunogenicity
Non-versatile (one type of cargo)	Versatile (multiple types of cargo)
Larger cargo capacity	Smaller cargo capacity
Complex manufacturing	Relatively easy production and scaling-up

The PEI is a cationic polymer that has been on the spotlight for nucleic acid delivery as an alternative to viral vectors. The PEI and PEI-derived polymers (>20 kDa) in high molecular weight form display multivalent binding to nucleic acids that lead to stable nanoparticles that can withstand membrane penetration [10,11]. However, they also display significant toxicity on sensitive human cells, although PEI cytotoxicity has been successfully reduced by modifying it with peptides, vitamins, amino acids, etc. [12–14]. The low molecular weight PEI (<2 kDa) is relatively non-toxic due to weaker cell membrane interactions but also unable to act as a carrier. Our studies have shown that lipid modifications on low molecular weight PEI can convert the non-

effective small molecular weight PEI into an effective carrier for a range of nucleic acids due to increased uptake of resultant nanoparticles, so that it can be safely used to deliver siRNA, pDNA and mRNA *in vitro* [10,15–21]. However, *in vivo* delivery efficiency of the modified PEIs for nucleic acids remained to be explored.

In this manuscript, we explore the siRNA delivery efficiency of a series of three lipid-substituted PEI-derived polymers, namely Leu-Fect A, B and C, which are commercially available. The polymers were designed to implement siRNA therapy for the hematological cancer leukemia and *in vitro* studies previously indicated effective encapsulation of siRNA into nanoparticles and robust delivery into leukemic cells [19,20]. Here, using 2 leukemia xenograft models, biodistribution and delivery to various organs were investigated to better assess the feasibility for clinical translation.

MATERIALS and METHODS

Materials. The lipopolymers (i.e., Leu-Fect line of transfection reagents) used in this study and Trans-Booster additive were prepared by RJH Biosciences Inc. (Edmonton, Canada). The reference transfection reagent Lipofectamine™ 2000 was from Invitrogen, a division of Thermo-Fisher (Walthman, MA). The MTT solvent dimethyl sulfoxide (DMSO) was obtained from SIGMA-ALDRICH (St Louis, MO). Cell culture medium Roswell Park Memorial Institute (RPMI), and penicillin (10,000 U/mL)/streptomycin (10 mg/mL) mixture were obtained from Thermo-Fisher (Walthman, MA). Fetal bovine serum (FBS) was purchased from VWR (Radnor, PA). SYBR Green I was purchased from Cambrex Bioscience (Rockland, MD). Whole blood for isolation of red blood cells (RBCs) were obtained from Canadian Blood Services (Vancouver, Canada). The RNAlater used for preservation of extracted RNA, Trizol® used in RNA extraction

and TaqMan™ MicroRNA Reverse Transcription Kit (#4366596) for cDNA synthesis were obtained from Thermo-Fisher Scientific (Walthman, MA). The MGB-TaqMan probes as well as forward and reverse primers for Bcr-Abl and FLT3 were also from Thermo-Fisher (Walthman, MA). The siRNAs used in this study were obtained from IDT (Coralville, IA) or from Biospring (Frankfurt, Germany). The sequences of the siRNAs were:

- BCR-Abl siRNA sense: rGrCrArGrArGrUrUrCrArArArArGrCrCrCrUrUTT; antisense: rArArGrGrGrCrUrUrUrUrGrArArCrUrCrUrGrCTT.
- FLT3 siRNA sense: rArUrGrCrUrArCrCrArArUrUrCrArArGrUrGrArArGrArUTA; antisense: rUrUrUrArCrGrArUrGrGrUrUrArArGrUrUrCrArCrUrUrCrUrArArU
- Negative Control siRNA sense: rGrCrGrUrArUrUrArUrArCrGrCrGrArUrUrArACG; antisense: rCrGrUrUrArArUrCrGrCrGrUrArUrArArUrArCGC

The consumables for the digital droplet PCR (ddPCR) on QX100 Droplet Generator (BioRad), ddPCR™ Supermix for Probes (#1863010), DG8™ Cartridges for QX200™/QX100™ droplet generator (#1864008) and droplet generation oil (#1863005) were from BioRad (Hercules, CA).

Particle Size and ζ-potential Measurement: Leu-Fect complexes with siRNA were prepared by mixing 46.9 µg of the Leu-Fect A/B/C with 6.25 µg of siRNA (carrier:siRNA weight ratio of 7.5:1), and diluted in 50 µL Phosphate Buffered Saline (PBS) at room temperature (RT). Complexes were incubated at RT for 30 min to allow complete binding and then diluted in 950 µL of PBS before being transferred to a Univette for particle size and ζ-potential measurement in a Litesizer 500® particle analyzer (Anton Paar).

Transmission Electron Microscopy (TEM): The complexes were prepared as described above. A total of 10 µL of suspension was dropped on top of a carbon-coated copper TEM grid and air dried for 10 mins at RT. For negative staining, uranyl acetate (1% w/v, 5 µL) was further added

on the copper grid and dried naturally overnight. The morphology of complexes was visualized by TEM using a JEOL JEM-2100 electron microscope.

Binding Assay: The complexes of siRNA were prepared by mixing 0.56 µg of siRNA with Leu-Fect A, B and C at different weight/weight ratios (see Results), and diluted in 50 µL of PBS. Complexes were transferred to a black-bottom 96-well plate and incubated at RT for 30 min. Then, 50 µL of SYBR Green 2X (in PBS) were added to each well and fluorescence was read in a fluorometer at an excitation/emission wavelength of 485 nm/527 nm. A control sample (100% free siRNA) was generated by diluting 0.56 µg of siRNA as in above without any carrier being added to it. The binding concentration required for 50% binding (BC_{50}) was calculated by fitting the fluorescence curves using a 4-parameter logistic regression. In addition, amount of unbound siRNA was assessed by loading the complexes onto a 1.2% agarose gel stained with ethidium bromide. The proportion of unbound siRNA was calculated using a reference of 100% free siRNA with no carrier.

Hemolysis Assay: Red blood cells (RBCs) were separated from the whole human blood (obtained from Canadian Blood Services, under an approved protocol) as per the Ficoll-Paque protocol [17]. In brief, the whole human blood was diluted with equal volume of HBSS. 20 mL of diluted blood was carefully layered over 15 mL of Ficoll-Paque plus and centrifuged 40 mins at 400 g. The bottom RBCs were collected and washed with HBSS before use. To assess for hemolysis caused by the complexes, 100 µL of Leu-Fect/siRNA complexes at various ratios were pipetted into a 96-well plate. Then, 100 µL of RBC in HBSS were added to each well. Plate was incubated at 37°C for 30 minutes and then centrifuged at 500 x g for 10 minutes. Supernatant was transferred to a

clean flat-bottom 96-well plate and absorbance was measured at 540 nm (Spectramax 250). A 100% hemolysis control was achieved by incubating RBCs with Triton X100 at a final concentration of 0.1% v/v, while incubation with HBSS served as negative control. The hemolytic activity percentage was calculated as follows:

$$\text{Hemolysis (\%)} = \frac{\text{Abs (test)} - \text{Abs (negative ctrl)}}{\text{Abs (positive ctrl)} - \text{Abs (negative ctrl)}} \times 100\%$$

Heparin Displacement Assay: The complexes of siRNA were prepared by mixing 2.8 µg of the indicated Leu-Fects with 0.56 µg of siRNA (ratio 5:1), diluted in 50 µL of PBS at RT. Complexes were transferred to a black-bottom 96-well plate and incubated at RT for 30 min. Then, 50 µL of heparin solution were added to each well to reach a final concentration from 0 to 100 U/mL for Leu-Fect A, and 0-20 U/mL for Leu-Fect B and Leu-Fect C. After 1h at RT, 100 µL of SYBR Green 2X (in PBS) were added to each well, and fluorescence was read in a fluorometer at an excitation/emission wavelength of 485 nm/527 nm. A 100% displacement control was done by using the same amount of siRNA without any Leu-Fect being added to it. Alternatively, amount of unbound siRNA was measured by agarose gel electrophoresis. The proportion of released siRNA was calculated using a reference of 100% free siRNA.

Cell Uptake by Flow Cytometry. The leukemia cell lines MV4-11 cells (acute myeloid leukemia) and K562 cells (chronic myeloid leukemia) were cultured at 37 °C with 5% CO_2 and saturated humidity with RPMI medium. The RPMI medium was supplemented with 10% fetal bovine serum (FBS) and 10 g/mL penicillin-streptomycin. Regular cell passage was executed when cells reached 75% confluency. For uptake studies, Leu-Fect/FAM-labeled siRNA complexes were prepared at different ratios. Reverse transfection was performed by incubating the FAM-labeled siRNA

complexes at a final concentration of 60 nM with MV4-11 or K562 cells at a density of 150,000 cell/mL. Complexes were pipetted first into 48-well plates, followed by the cell suspension. Lipofectamine^{TM} 2000 was used as a reference reagent and siRNA complexes were prepared at the manufacturer recommended reagent/siRNA ratio of 2:1. FAM-siRNA uptake was assessed after 24 hours of reverse transfection by flow cytometry using an Attune NxT Flow Cytometer (Thermo-Fisher). Data was analyzed using the Attune NxT acquisition and analysis software.

Confocal Microscopy: MV4-11 cells were reverse transfected at a density of 150,000 cells/mL with 60 nM of FAM-labeled siRNA for 24 hours using Leu-Fect A, B and C at a 7.5:1 Leu-Fect:siRNA ratio. After 24 hours of incubation, cells were fixed with 4% paraformaldehyde and stained with 1 μg/mL DAPI solution for 15 min. Cells were washed and mounted on glass coverslips. Imaging was done on a LSM 710/Observer.Z1 laser scanning confocal microscope using a 63X/oil objective. Images were processed and analyzed using the NIH open-source software Image J.

MTT Assay: To assess acute toxicity caused by the carriers, the leukemic MV4-11 and K562 cells were incubated with 60 nM of control (scrambled) siRNA, complexed with Leu-Fect A, B and C at various Leu-Fect/siRNA ratios for 24 h at 37°C. Then, MTT reagent was added to the wells to a final concentration of 0.5 mg/mL and incubated at 37°C for 2h. MTT-containing media was removed by centrifugation and aspiration, and cells were lysed using 100 μL of pure DMSO. Absorbance was read at 570 nm and proportion of survival was calculated based on absorbance of untreated cells.

Animal Husbandry: All animal studies were approved by the University of Alberta Health Sciences Approval Board. Animals were maintained following the Canadian Council on Animal Care (CCAC) guidelines. Immunodeficient triple mutant NCG (NOD CRISPR Prkdc, Il2r, gamma/NjuCrl) mice were purchased from Charles River (Quebec, QC) and were allowed to acclimate for 1-2 weeks in an ABL-2 facility, caged 4-5 animals per cage. Food and water were provided *ad libitum*. Animals were euthanized using a CO_2 chamber according to the protocols stablished by CCAC and the University of Alberta Research Ethics Board.

Establishment of K562 or MV4-11 Tumors. Mice were anesthetized using isoflurane vapour and a Patterson Scientific Model SAS3 rodent anesthesia machine. Human K562 or MV4-11 cells were injected subcutaneously into the right thigh of each mouse at 2.5-5 $x10^6$ cells per mouse, suspended in 200 µL of RPMI-1640 medium. Tumor growth was assessed every 3 days by external inspection, which usually became visible a week after injection. The length (l) and width (w) of the tumors were measured using a caliper and tumor volume was calculated based on the formula: volume = length (l) x width $(w)^2$ x 0.5. The animals have undergone injections of siRNA complexes once the tumors reached a volume of 50-100 mm^3.

Preparation of BCR-Abl siRNA containing Lipid Nanoparticles (LNPs)

BCR-Abl siRNA-containing LNPs were synthesized by micromixing lipid solutions with an aqueous solution of siRNA duplexes, following a previous report with slight modifications [22]. In brief, D-Lin MC3 DMA (TargetMol. Wellesley Hills, MA), DSPC (Avanti Polar Lipids, Alabaster, AL), cholesterol (Sigma-Aldrich, St. Louis, MO), and DMG-PEG-2000 (Avanti Polar Lipids, Alabaster, AL) were dissolved in ethanol at a mole ratio of 50:10:38.5:1.5, respectively.

BCR-Abl siRNA was prepared in 25 mM acetate buffer solution at pH 4.0. Both siRNA solution and lipid mixture were then injected into microfluidic mixer (NanoAssemblr™ 1.5 by Precision Nanosystems, BC, Canada) at a 3:1 volume with a flow rate ratio of 3 mL/min aqueous, and 1 mL/min ethanol. The resultant siRNA/LNPs were immediately dialyzed using a 12-14kD dialysis tubing (Thermo-Fisher, Waltham, MA) against a buffer (pH 6.7) containing 50 mM sodium citrate and 50 mM MES for 4 hrs. Subsequently, an overnight dialysis was carried out in PBS at pH 7.4 (Sigma- Aldrich, St. Louis, MO). siRNA/LNPs were then filtered through a 0.2 µm filter (Thermo-Fisher, Waltham, MA) for further use. The entire procedure was conducted at room temperature. LNPs Z-average was assessed by Dynamic Light Scattering (DLS) using a Litesizer 500® particle analyzer (Anton Paar) set at 25 °C and measurement angle of 173°.

***In vivo* siRNA Administration:** Mice were injected with complexes formed by mixing 187.5 µg of Leu-Fect A, B or C with 25 µg of either control (scramble), FLT3 or BCR-Abl siRNA (ratio 7.5:1), diluted in 200 µL of RPMI medium. Complexes were incubated at RT for 30 min before being injected via tail vein as a single injection.

Quantification of siRNA in Organs: After euthanasia, mice were dissected and organs were preserved in 250-500 mL of RNAlater at -80 °C. The amount of siRNA delivered into tumor and other tissues was measured by first isolating total RNA from a fraction of tissue (10-20 mg), which was homogenized in a RNase-free microcentrifuge tube containing 500 mL of Trizol® following the manufacturer's instructions. The concentration and integrity of extracted RNA was examined by spectrophotometry (NanoDrop™, Thermo-Fisher Scientific). Next, reverse transcription was performed using a proprietary custom-designed stem-loop primer from Thermo-Fisher Scientific

or an in-house designed stem loop primer: BCR-Abl: 5' GTC GTA TCC AGT GCA GGG TCC GAG GTA TTC GCA CTG GAT ACG ACA AAA GG 3'; FLT3: 5' GTC GTA TCC AGT GCA GGG TCC GAG GTA TTC GCA CTG GAT ACG ACT AAT CT 3' and the TaqMan™ MicroRNA Reverse Transcription Kit according to the protocol from the manufacturer, using 10 ng of total RNA as template. Once the cDNA was synthesized, the number of copies of BCR-Abl or FLT3 siRNA was measured by one of two methods:

1) ddPCR: For this, the equivalent of 0.0001 to 0.1 ng of cDNA were amplified using proprietary custom-designed MGB-TaqMan probes as well as forward/reverse primers, or the following oligonucleotides: BCR-Abl Fwd primer: 5' CAC GCA GCA GAG TTC AAA 3'; BCR-Abl MGB fluorescent probe: /56-FAM/CTG GAT ACG ACA AAA GG /3MGB-NFQ/; FLT3 Fwd primer: 5' CAC GCA ATG CTA CCA ATT C 3'; FLT3 MGB fluorescent probe: /56-FAM/CA CTG GAT ACG ACT AAT CTT C/3MGB-NFQ/; Universal Reverse Primer: 5' CCA GTG CAG GGT CCG AGG TA 3'. The cDNA templates, primers and probes were mixed with ddPCR™ Supermix for Probes and droplets were generated in DG8™ Cartridges for QX200™/QX100™ Droplet Generator using Droplet Generation Oil for Probes and a QX100 Droplet Generator. Droplets were read in a QX100 Droplet Reader and data collection/analysis were done using QuantaSoft Software, v1.7 (BioRad).

2) Quantitative Real-Time PCR (qPCR): A standard curve was created with BCR-Abl or FLT3 siRNAs, complexed with the appropriate Leu-Fect at a ratio of 7.5:1 Leu-Fect/siRNA. Starting concentration was 1 nM, followed by 1:5 serial dilutions for up to 8 points. For the qPCR reaction, 1 uL of cDNA sample or standard was used in combination with TaqMan Universal Master Mix. Proprietary custom-designed MGB-TaqMan probe, as well as forward and reverse primers were used. Thermocycling parameters were followed as per manufacturer's instructions, and

concentration of BCR-Abl or FLT3 siRNAs was calculated by extrapolating Ct values of the unknowns to the standard curve.

Statistical Analysis: Statistical analysis was performed in GraphPad Prism Software (Version 8.0.2). Statistical significances were analyzed by student t-test when comparing two groups. When comparison was made between 3 or more groups, ordinary One-way ANOVA followed by a Tukey's multiple comparisons test, or Kruskal-Wallis followed by Dunn's multiple comparison tests was performed. Alpha was set as 0.05 across the studies.

RESULTS

Physical properties of complexes made with siRNA and Leu-Fects

The surface charge density, given by the ζ-potential, can directly affect how a nanoparticle interacts with biological elements, such as serum proteins and cellular membranes [23,24] and thus impact its delivery capacity. It was previously shown that efficacious nanoparticles made with lipid-substituted PEI-derived polymers have positive ζ-potentials [19,25]. As expected, the siRNA complexes made with Leu-Fect A, B and C show positive ζ-potentials of +24.0, +19.1 and +30.8 mV, respectively (Fig. 1A), consistent with previous findings. In terms of particle size, the siRNA complexes made with Leu-Fect A and Leu-Fect C showed sizes averaging between 133 nm and 194 nm, respectively. Conversely, Leu-Fect B resulted in nanoparticles averaging 405 nm (Fig. 1B). The size of siRNA complexes was further confirmed by the TEM (Fig. 2). Despite the differences, the sizes of siRNA complexes made with the three carriers fall within the typical range of other gene delivery nanoparticles, such LNPs [26]. To investigate whether the presence or absence of salts affects the ζ-potential or size of the complexes, we complexed Leu-Fect A with

siRNA in either pure water or PBS. In the absence of ions, we observed that the ζ-potentials of complexes prepared in water was significantly higher than particles prepared in PBS. On the other hand, the particle size showed a non-significant difference between the solvents (Supp Fig. 1).

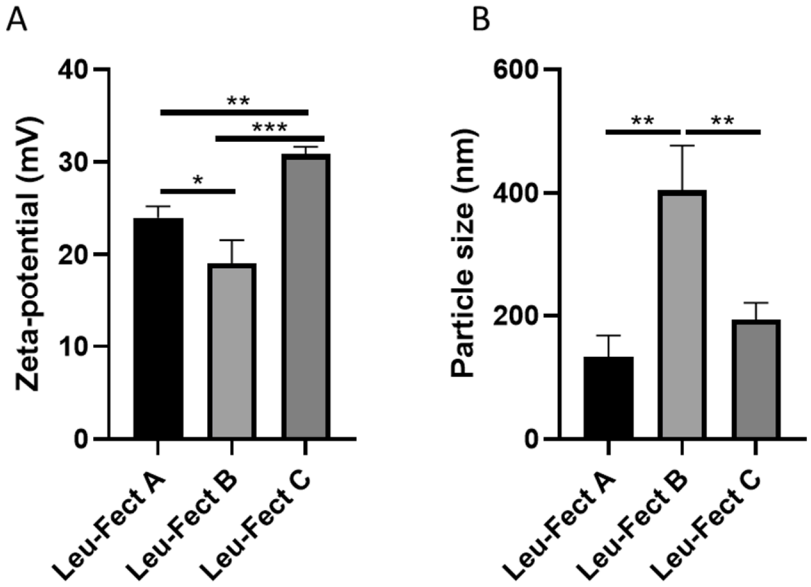

Figure 1: ζ-potential and particle size of siRNA complexes using lipid-substituted PEI polymers: ζ-potential (**A**) and particle size (**B**) of nanoparticles made using siRNA and the carriers Leu-Fect A, Leu-Fect B and Leu-Fect C. ζ-potential for all three siRNA complexes was in the range of 19-31 mV. Particle size was significantly bigger for particles made with siRNA and Leu-Fect B (*=p<0.05; **=p<0.01; ***=p<0.001. ANOVA followed by Tukey's multiple comparisons test).

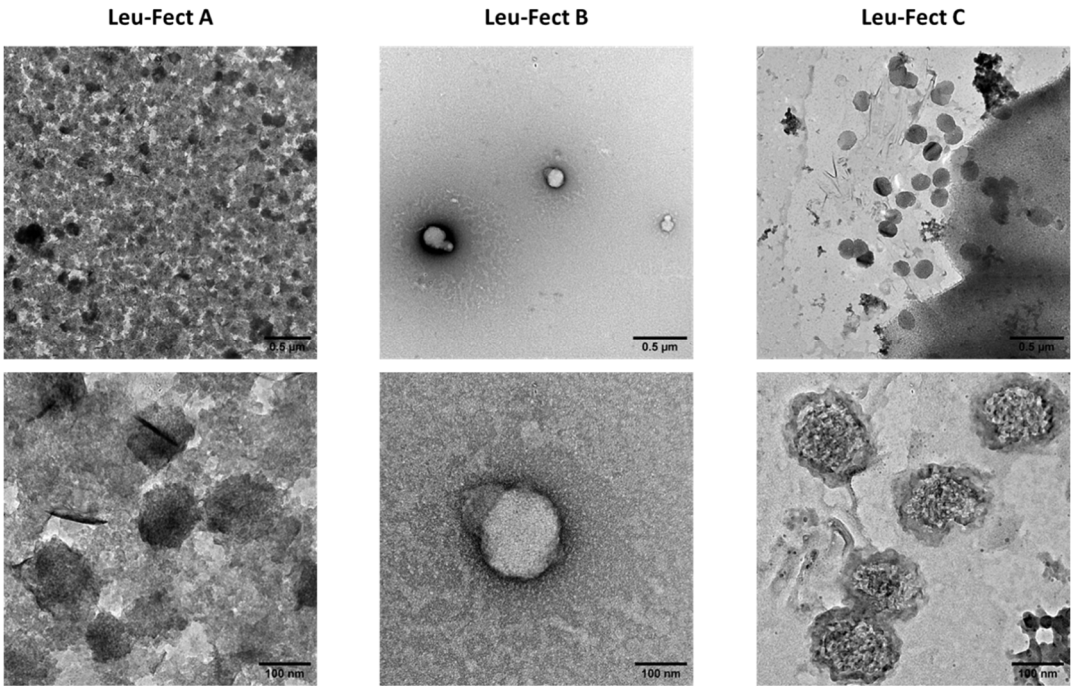

Figure 2: TEM of siRNA complexes with Leu-Fect carriers: Representative images of complexes made with siRNA and Leu-Fect A, Leu-Fect B and Leu-Fect C (from left to right). The lower pictures are from high magnification images.

Binding Capacity of Leu-Fect Carriers

To assess the siRNA binding capacity of the carriers, complexes were prepared using a variable ratio of Leu-Fect to siRNA and the free siRNA was measured after the binding. Amongst the three lipopolymers, Leu-Fect A has the highest affinity with a BC_{50} of 0.33±0.04, while Leu-Fect B and Leu-Fect C showed BC_{50} values of 0.54±0.03 and 0.63±0.03, respectively (Fig. 3A). To confirm our findings, we used agarose gel electrophoresis to assess the amount of free siRNA after complexation at different Leu-Fect/siRNA ratios. As before, Leu-Fect A showed greater affinity for siRNA. However, we observed that Leu-Fect B showed unbound siRNA even at a higher carrier/siRNA ratio than the Leu-Fect C (Fig. 3B). This could be due to the electrical current in the gel electrophoresis set-up exhibiting an extra force and uncovering a weaker affinity of Leu-

Fect B, which was only observable when the binding was challenged by external forces (as in gel electrophoresis).

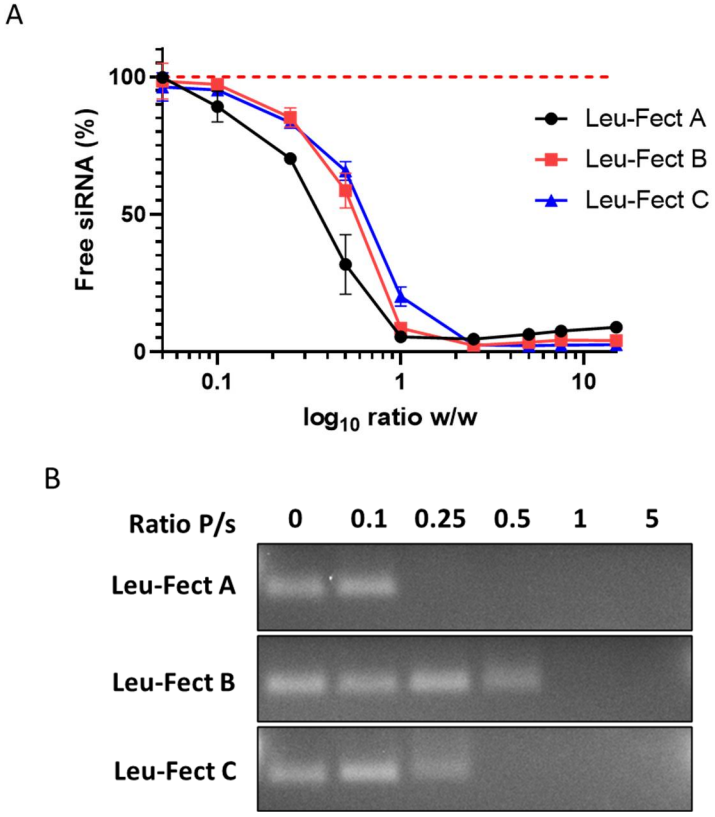

Figure 3: Binding assay of siRNA by Leu-Fect carriers: (A) Free siRNA was determined after complexation with various amounts of Leu-Fect, represented as ratio of the carrier to siRNA (w/w). Leu-Fect A showed a higher affinity (BC_{50} = 0.33 ±0.04), followed by Leu-Fect B (BC_{50} = 0.54±0.03) and Leu-Fect C (BC_{50} = 0.63±0.03). **(B)** Agarose gel electrophoresis showing unbound siRNA when siRNA/Leu-Fect complexes are prepared at different ratios. Free siRNA with no polymer was loaded as control (Ratio P/s = Ratio of carrier to siRNA).

To further explore the binding affinity of lipopolymers, complexes were exposed to increasing concentrations of heparin to assess their propensity for dissociation. In line with the previous observations, complexes made with Leu-Fect B were susceptible to dissociation by heparin at lower concentrations than the other two lipopolymers with a DC_{50} value of 2.03±0.07 U/mL, while complexes made with Leu-Fect C had a DC_{50} value of 5.35±0.15 U/mL (Fig. 4A). Interestingly, complexes made with Leu-Fect A were very resistant to heparin displacement, not reaching to

50% dissociation even at high heparin concentrations of 100 U/mL (Fig. 4A). These findings were in line with agarose electrophoresis results. While heparin concentrations of 5 U/mL dissociated all of the siRNA complexed with Leu-Fect B or C, complexes prepared with Leu-Fect A required much higher concentrations of heparin to produce similar dissociations (Fig. 4B).

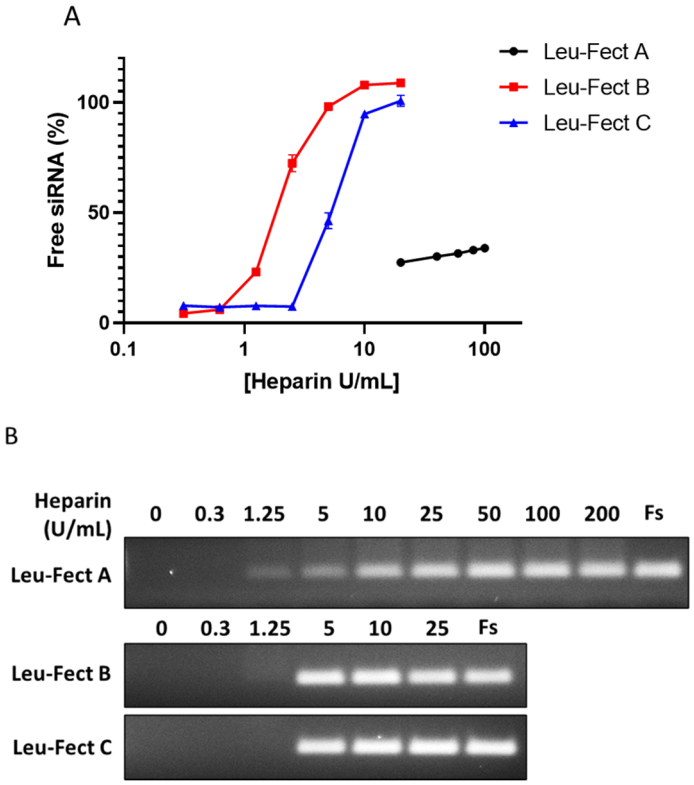

Figure 4: Heparin displacement assay of siRNA complexes: (A) Once the siRNA complexes were formed, siRNA was displaced using various concentrations of heparin. Free siRNA was measured after displacement using SYBR green fluorescence. Leu-Fect B (DC_{50} = 2.0±0.1 U/mL) and Leu-Fect C (DC_{50} = 5.3±0.1 U/mL) show effective displacement with heparin, while high concentrations of heparin did not cause siRNA displacements in complexes made with Leu-Fect A. **(B)** Agarose gel electrophoresis showing unbound siRNA when displaced from the siRNA complexes by different concentrations of heparin. Free siRNA (Fs) with no polymer is loaded as control.

Since the lipopolymers were designed for delivery of siRNAs *in vivo,* it is important to assess whether the serum components could dissociate and/or digest the siRNA when complexed with the carriers. For this, we prepared the complexes and incubated them with FBS up to a final FBS concentration of 50%. Agarose gel electrophoresis showed that FBS did not cause dissociation of

the siRNA complexes (Fig. 5A), since no free siRNA was detected on the gel. To rule out the possibility of siRNA degradation (hence lack of free siRNA), complexes were resuspended in 25-50% of FBS, incubated for 24 h at 37°C and siRNA within the complexes was released using heparin (final concentration: 200 U/mL). In contrast to free siRNA that was totally degraded by the FBS, complexation with the lipopolymers protected the siRNA against degradation (Fig. 5B). It was interesting to note that FBS contributed to the release of siRNA form Leu-Fect A and Leu-Fect B complexes (i.e., higher recovery of siRNA in the presence of 50% FBS), but not from the Leu-Fect C complexes (Fig. 5B).

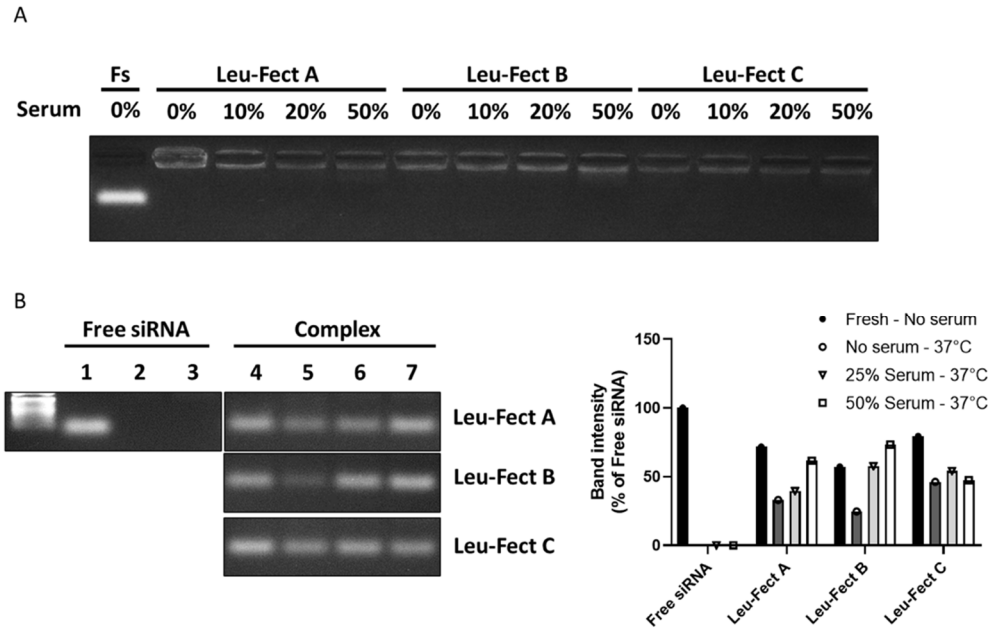

Figure 5: Effect of serum siRNA complexes. (A) Once the siRNA complexes were formed, they were exposed to increasing concentrations of FBS for 1h. FBS was not able to dissociate any detectable siRNA from the complexes. Free siRNA (Fs) was loaded onto the gel as positive control. **(B)** The siRNA complexes are resistant to serum-mediated degradation, while free siRNA is not. Presence of serum also facilitates heparin-mediated siRNA dissociation. Unless otherwise stated, samples were incubated at 37° for 24 h. 1. Free siRNA freshly diluted; 2. Free siRNA + 25% serum; 3. Free siRNA + 50% serum; 4. Complex freshly prepared; 5. Complex – no serum; 6. Complex + 25% serum; 7. Complex + 50% serum.

In vitro siRNA Uptake by Leukemic Cells

To assess the cellular siRNA delivery capacity of the chosen carriers, we delivered FAM-labeled siRNA (60 nM) into MV4-11 and K562 cells, models of acute and chronic amyloid leukemia, respectively. Assessment of transfection efficiency was performed by flow cytometry. In MV4-11 cells, Leu-Fect A was more efficient in delivering the FAM-siRNA at all carrier/siRNA ratios when compared to Leu-Fect B and C. Moreover, at most carrier/siRNA ratios, we found that all Leu-Fect carriers generated higher FAM-siRNA uptake compared with a commercial lipofection reagent Lipofectamine™ RNAiMAX. Similar results were obtained when K562 cells were used for uptake studies instead of MV4:11 cells (Fig. 6).

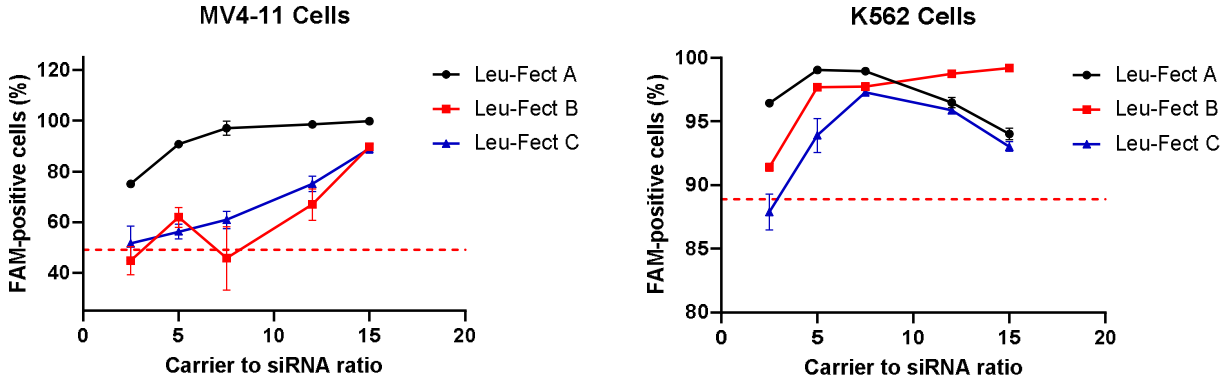

Figure 6: In vitro uptake of FAM-labeled siRNA by flow cytometry. MV4-11 cells (left) and K562 cells (right) were treated with 60 nM of FAM-siRNA at various polymer/siRNA ratios. Proportion of FAM-positive cells was measured by flow cytometry 24h after transfection. Horizontal red line represents uptake obtained using Lipofectamine™ RNAiMAX at a reagent/siRNA ratio 2:1.

To corroborate that FAM-siRNA was in fact being internalized by the leukemia cells, MV4-11 were transfected with Leu-Fect or Lipofectamine™ RNAiMAX complexes of FAM-siRNA. Cells were fixed and stained with DAPI, and analyzed by confocal microscopy. Images showed a clear intracellular localization of FAM-siRNA in all cells transfected with the Leu-Fect complexes, and a particularly high uptake in cells transfected with Leu-Fect A was observed (Fig. 7 and Supp. Fig. 2), supporting the results obtained using flow cytometry.

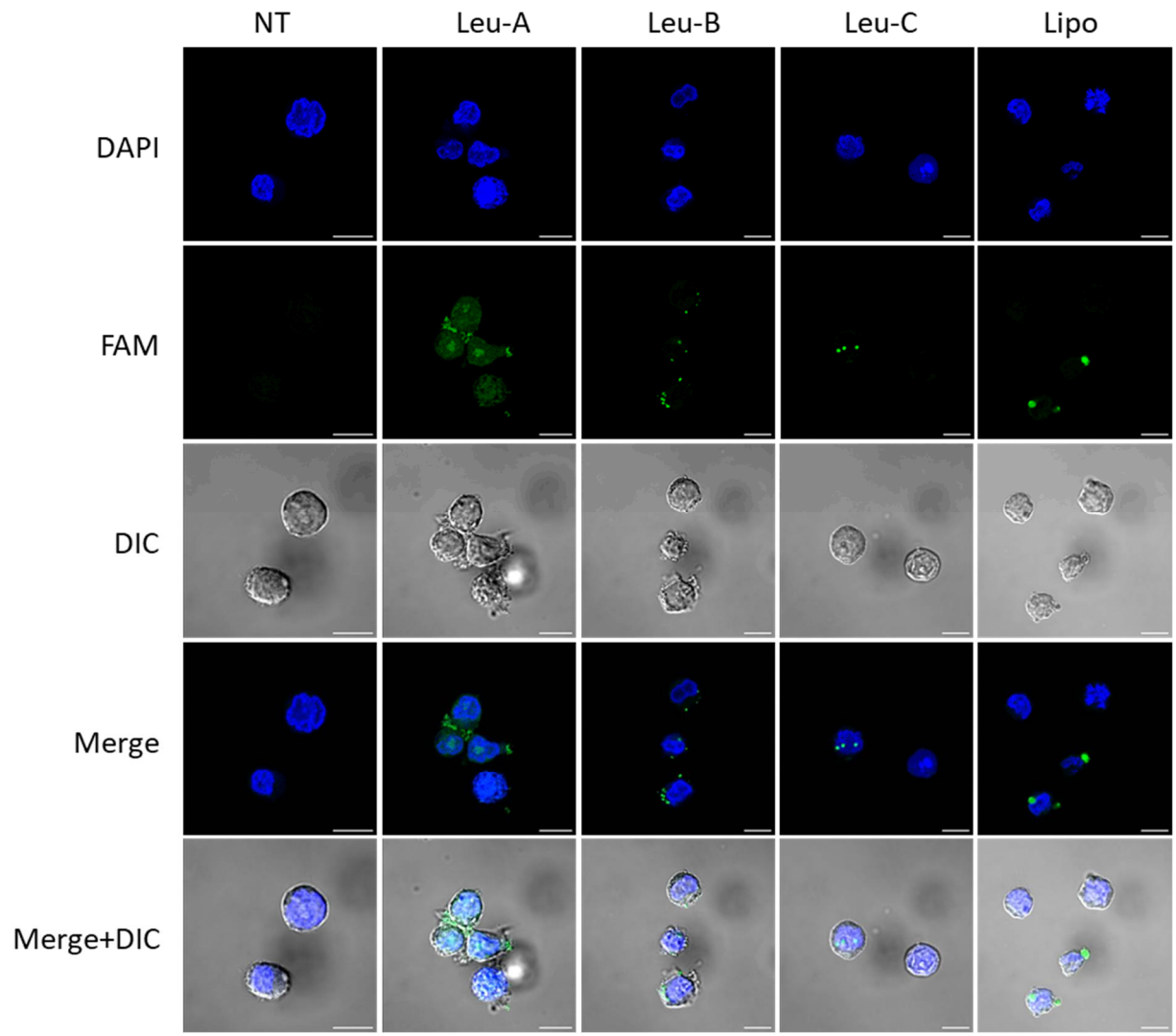

Figure 7: In vitro uptake of FAM-labeled siRNA by confocal microscopy. Representative images obtained by confocal microscopy of MV4:11 cells treated with 60 nM of FAM-siRNA complexes at a 7.5:1 carrier/siRNA ratio. Lipofectamine™ RNAiMAX complexes were prepared at a reagent/siRNA ratio 2:1. NT: No treatment.

Toxicity of Leu-Fect Carriers

To evaluate the potential toxicity of Leu-Fect carriers, MV4-11 and K652 cells were treated with scrambled (no target) siRNA complexes at different carrier/siRNA ratios, and cell viability was compared to complexes prepared by the leading lipofection reagent. In MV4-11 cells, Leu-Fect A and B toxicity increased with increasing carrier/siRNA ratio, but even at high ratios, the observed

toxicity was lower than the lipofection reagent. Conversely, toxicity of complexes formulated with Leu-Fect C at ratios 5:1 and 7.5:1 was comparable to lipofection reagent toxicities, and it became more toxic when used at higher ratios (Fig. 8A). Similar outcomes were observed with the K562 cells when are treated with the same complexes (Fig. 8B).

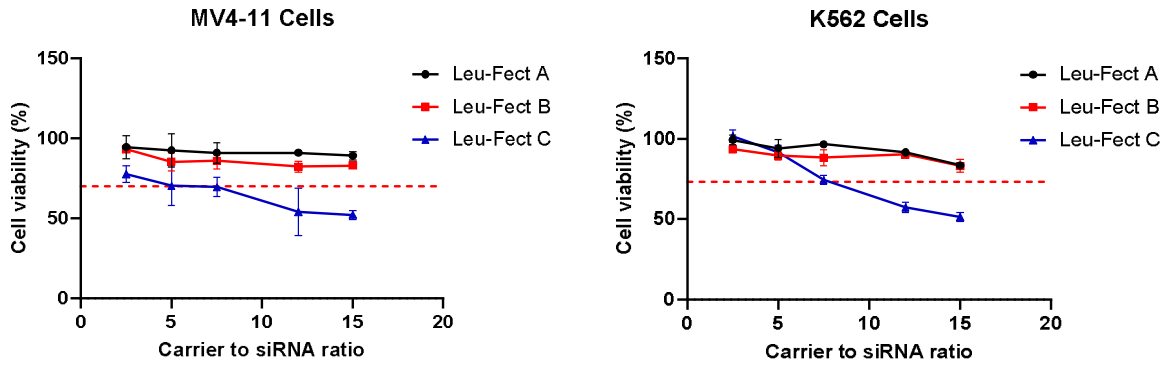

Figure 8: Direct toxicity of siRNA complexes with Leu-Fect. MV4-11 cells (left) and K562 cells (right) were treated with 60 nM of negative control (no target) siRNA at various carrier/siRNA ratios. Cell viability was assessed using the MTT assay. Horizontal red line represents cell viability after using siRNA complexes of Lipofectamine™ RNAiMAX at a reagent/siRNA ratio of 2:1.

The hemolytic effect of the Leu-Fect carriers was also tested using human RBCs isolated from whole blood. Leu-Fect A and Leu-Fect B, at carrier/siRNA ratios up to 7.5:1 showed ~5% of hemolysis, which increased with increasing amount of the carrier. Instead, Leu-Fect C showed significantly higher rates of hemolysis than Leu-Fect A and B at similar ratios (Fig. 9).

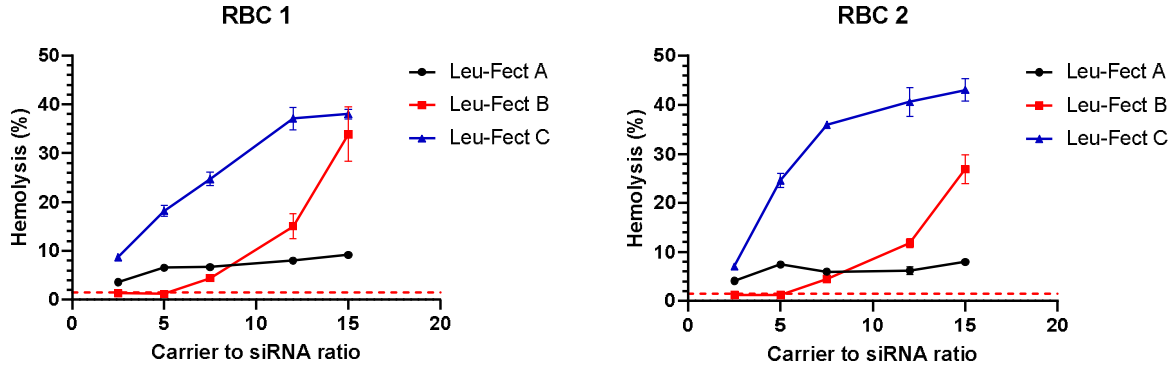

Figure 9: Hemolysis caused by the siRNA complexes of Leu-Fect carriers. Two separate human RBC samples were treated with siRNA complexes at various carrier/siRNA ratios. Hemolysis was measured by absorbance at 540 nm. Horizontal red line represents hemolysis caused by the Lipofectamine™ RNAiMAX

complexes at the reagent/siRNA ratio of 2:1. Total hemolysis control (100%) was generated by treating RBCs with Triton X-100 at 0.1% v/v.

Biodistribution of siRNA in CML Xenograft Model

In previous studies, we evaluated the antitumoral efficacy of systemic injections of BCR-Abl siRNA complexes in an *in vivo* model of CML. We found that treating mice carrying CML xenografts with BCR-Abl siRNA complexes caused a significant reduction in tumor growth when compared to Ctrl siRNA delivered by Leu-Fect C [27]. For this study, the biodistribution of siRNA to different organs were investigated using the Leu-Fect C in a mouse model bearing CML xenografts. The NCG mice were injected subcutaneously with 2.5 x 10^6 K625 cells in one of the hindlimbs. Once tumors were visible, mice received 5 IV injections, every second day, of either vehicle (RPMI medium) or 25 µg of BCR-Abl siRNA or Ctrl siRNA complexed with Leu-Fect C at a 7.5:1 Leu-Fect/siRNA ratio. The weight ratio was selected based on efficacy data previously published [16,27], as well as our *in vitro* direct toxicity and hemolysis data shown in figures 8 and 9. Two days after the last injection, the grafted tumors and major organs were collected for quantification of BCR-Abl siRNA in the tissues, using stem-loop RT-PCR followed by ddPCR. First, we tested the specificity of the stem-loop primer designed to detect the BCR-Abl siRNA, represented as number of copies per ng of total RNA used in the reaction. In tumors, lungs and hearts of animals treated with BCR-Abl siRNA complexes, significant amounts of BCR-Abl siRNA were detectable, while organs obtained from animals treated with vehicle or Ctrl siRNA showed considerably less signal, suggesting that stem-loop RT-PCR followed by ddPCR is a method of high sensitivity and specificity for the assessment of *in vivo* siRNA biodistribution (Supp. Fig 3). Importantly, the amount of BCR-Abl siRNA detected was higher in lungs, liver and spleen, and the quantification revealed strikingly similar numbers regardless of whether the

number of siRNA copies was normalized over amount of total RNA used in the reaction, or by mass of tissue utilized in the preparation (Supp. Fig 4). The latter was particularly important when analyzing siRNA biodistribution to tissues whose weight is not easy to obtain and register (e.g., blood or bone marrow).

We next compared the performance of Leu-Fect A, B and C in delivering siRNAs to major organs and the xenografts. After a single 25 μg of BCR-Abl siRNA injection, either free or complexed with Leu-Fect carriers, organs and xenograft tumors were collected after 48 h for quantitation using the stem-loop RT-PCR followed by ddPCR. As expected, free siRNA was not effectively delivered when compared to siRNA formulated with the Leu-Fect carriers (i.e., siRNA levels equivalent to background levels in the absence of a carrier), presumably due to a combination of factors including degradation and poor transport across membranes (Fig. 10). Furthermore, with exception of the heart, Leu-Fect A showed the highest average delivery among the organs. Leu-Fect C showed higher average biodistribution than the Leu-Fect B in xenograft tumor, blood, and lung, although these differences were not statistically significant due to the high variability across animal subjects. As observed before, the organs that showed the highest biodistribution of BCR-Abl siRNA were lung, liver and spleen (Fig. 10).

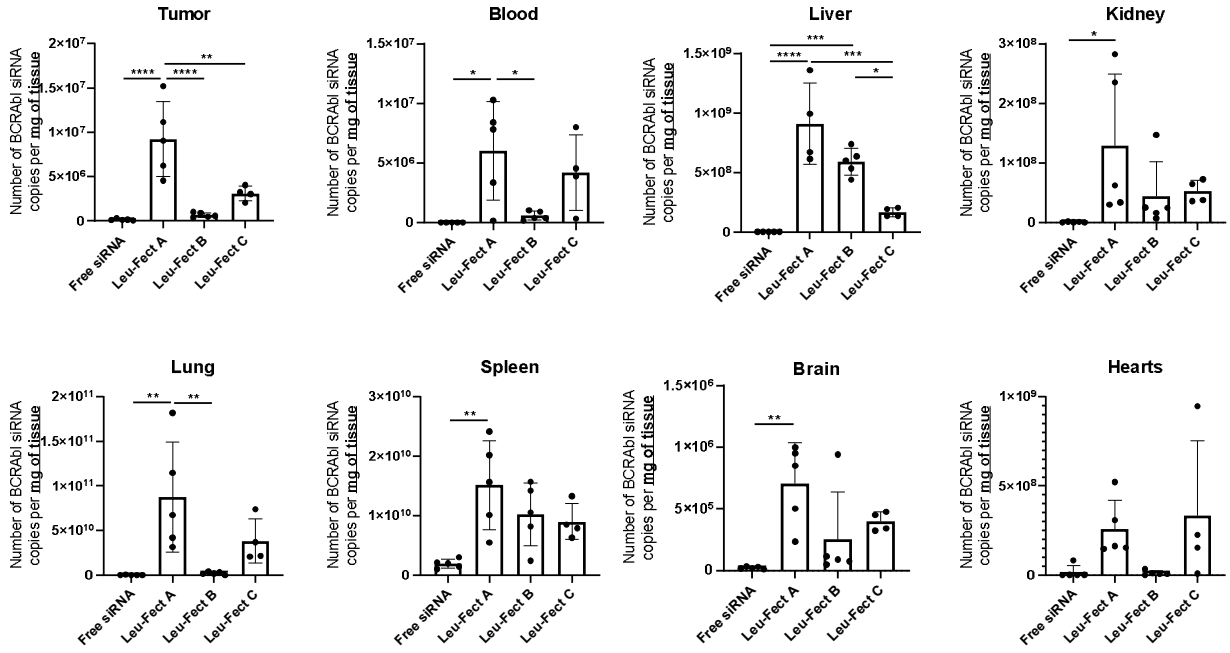

Figure 10. Biodistribution of siRNA in different organs. The amount of BCR-Abl siRNA in the tissues collected after 48 hours from mice injected with either free siRNA or complexed with Leu-Fect A, B or C, was expressed as number of copies per mg of tissue. Statistical analysis was performed using Ordinary One-way ANOVA followed by a Tukey's multiple comparisons test, comparing all columns to each other (****=p<0.0001; ***=p<0.001**=p<0.01; *=p <0.05).

Next, we compared the biodistribution of BCR-Abl siRNA using Leu-Fect A vs LNPs. The CML xenograft model was prepared as before and, once tumors were established, mice were subjected to a single injection with either vehicle (RPMI medium), 25 µg of BCR-Abl siRNA/Leu-Fect A complex (ratio of carrier/siRNA 7.5:1), or with 7 µg BCR-Abl siRNA/LNPs via tail vein. Lower amount of injection was necessary due to low encapsulation efficiency in LNPs in the maximal volume that could be injected IV (Supp. Fig. 5). Mice were euthanized 24 h or 7 days later, when organs and the xenograft tumors were collected for siRNA content analysis by ddPCR. Results showed that, after normalizing by the amount of siRNA injected, siRNA delivery by Leu-Fect A was significantly higher than LNPs into tumor, spleen, and liver after 24 hours of injection (Fig. 11). After 7 days, mice that were injected with BCR-Abl siRNA/Leu-Fect A complexes still showed considerable amounts of siRNA within bone marrow, spleen, and liver, while mice

injected with BCR-Abl siRNA/LNPs show almost undetectable levels of siRNA in these organs (Fig. 11).

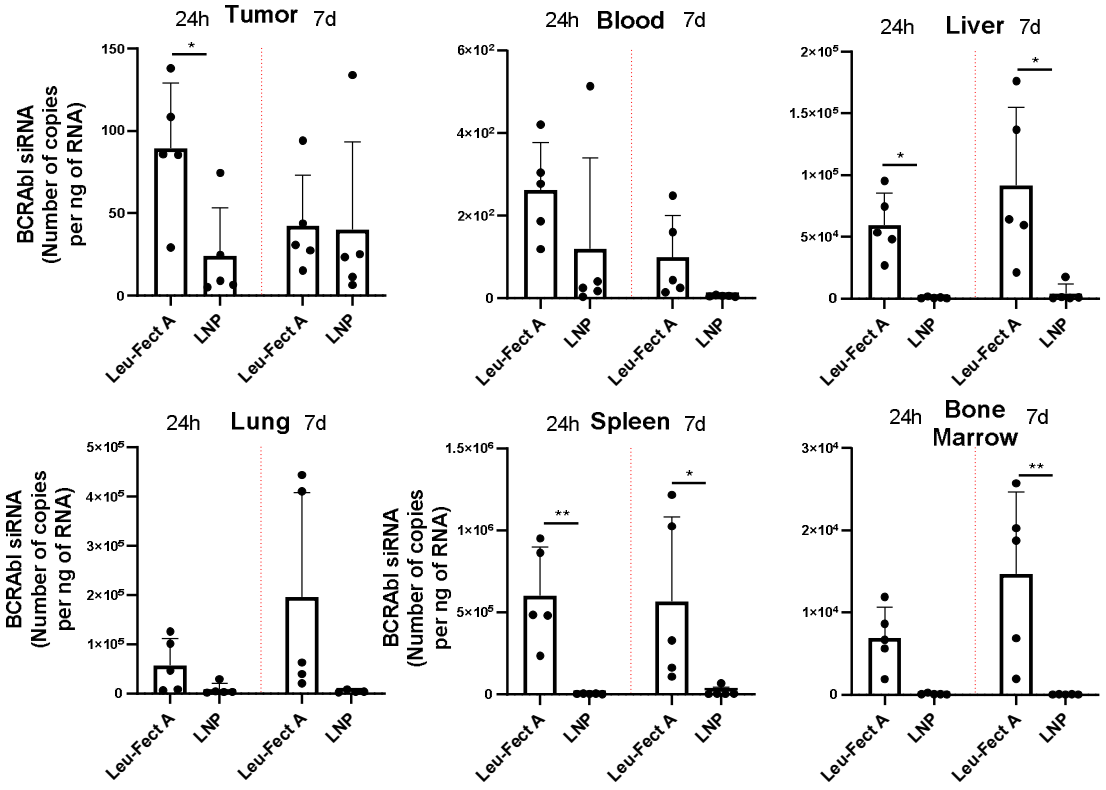

Figure 11: Comparison of biodistribution between Leu-Fect A or LNP delivered siRNA. The extent of BCR-Abl siRNA in different tissues was quantitated after collection from mice injected with either siRNA complexed with Leu-Fect A or encapsulated in LNPs after 24 hours or 7 days, expressed as number of copies per ng or RNA. (Kruskal-Wallis test, followed by Dunn's multiple comparisons test comparing Leu-Fect A vs LNPs. **=p<0.01; *=p <0.05).

Consistently with a high delivery of BCR-Abl siRNA into the xenograft tumor using Leu-Fect A, we found a significant decrease in the relative expression of tumoral BCR-Abl mRNA in animals treated with BCR-Abl siRNA/Leu-Fect A complexes in comparison with animals injected with vehicle only, after 24 hours of treatment (Fig. 12A). Any conclusion about the difference in silencing between Leu-Fect A an LNPs was considered not appropriate due to the difference in the total amount of siRNA injected between the 2 groups (data not shown). After 7 days of injection,

when the silencing effect has passed, we observed an increase in the relative expression of BCR-Abl in Leu-Fect A-treated mice, presumably due to a compensatory mechanism (Fig. 12B).

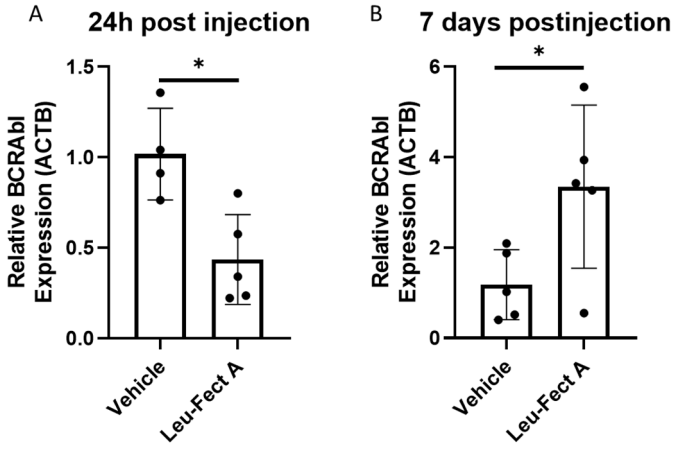

Figure 12: Comparison of BCR-Abl expression in mice treated with Leu-Fect A complexes. Analysis of the relative expression of BCR-Abl mRNA using actin B (ACTB) as housekeeping gene, in xenograft tumors collected from mice injected with either siRNA complexed with Leu-Fect A or vehicle after 24 hours (**A**) or 7 days (**B**) post-injection (* = $p<0.05$; Kruskal-Wallis followed by with Uncorrected Dunn's test).

Biodistribution of siRNA in AML Xenograft Model

We next investigated whether the biodistribution of other siRNAs were similar to the BCR-Abl siRNA, but also whether we could use the more common TaqMan qPCR, considering that the availability of ddPCR is not as widespread. For this, NCG mice were used to establish MV4-11 AML xenografts and an siRNA against oncogenic FLT3 was utilized for assessment of biodistribution. Once tumors were visible, mice received four IV injections every third day of either vehicle (RPMI medium) or 25 µg of FLT3 siRNA or Ctrl siRNA complexed with Leu-Fect B. Three days after the last injection, xenograft tumor and major organs were collected for quantification of FLT3 siRNA, using stem-loop RT-PCR followed by TaqMan qPCR. Contrary to the ddPCR, TaqMan qPCR requires a standard curve with changing concentrations of the target siRNA. To investigate the effect of carriers on the standard curve, we used the xenograft tumor RNA to run a stem-loop PCR followed by TaqMan qPCR using two standard curves: with free

siRNA or complexed with Leu-Fect B. We confirmed that the presence of Leu-Fect reagent in the qPCR reaction dramatically altered the standard curve (Supp. Fig. 6A) and as a result, quantitation of the unknown samples based on a standard curve might be affected with the presence of the carrier (Supp. Fig. 6B). It's worth to mention that such a shift in standard curves would affect absolute quantitation but not relative quantitation since the slope was almost identical. Furthermore, as with ddPCR, the TaqMan qPCR approach detected specifically the FLT3 siRNA, since no signal was present in the tumors of vehicle or Ctrl siRNA treated animals (Supp. Fig 6B).

We next compared the dynamic range of both techniques by running a standard curve made out of an initial concentration of 1 nM of FLT3 siRNA and 7 serial 1:5 dilutions in the presence of Leu-Fect B carrier. In the case of ddPCR, we observed an S-shaped resulting curve with loss of linearity in both the extremes of the concentration curve. Conversely, in TaqMan qPCR, linearity is maintained throughout the entirety of the standard curve (Supp. Fig. 7A, 7B).

Once the ideal conditions for TaqMan qPCR were established, the FLT3 siRNA content was measured in major organs. Since we already established that the probe was specifically detecting FLT3 siRNA and not Ctrl siRNA, only one random animal was run from NT and Ctrl siRNA groups when measuring siRNA content outside of the xenograft tumor. Spleen, liver and lung were once again the organs with the highest concentration of FLT3 siRNA, while tumor, heart and kidney were the organs with the lowest concentration (Fig. 13), which was in line with our previous results in the CML model with BCR-Abl siRNA.

Lastly, in order to further confirm if TaqMan qPCR was accurate in measuring the amount of siRNA in a particular tissue, samples obtained from the heart were also run using ddPCR. We found a strong correlation between the amount of siRNA detected by TaqMan qPCR and ddPCR

(Supp. Fig 8), confirming that both techniques, although different in some features, are of use when studying *in vivo* biodistribution of siRNAs.

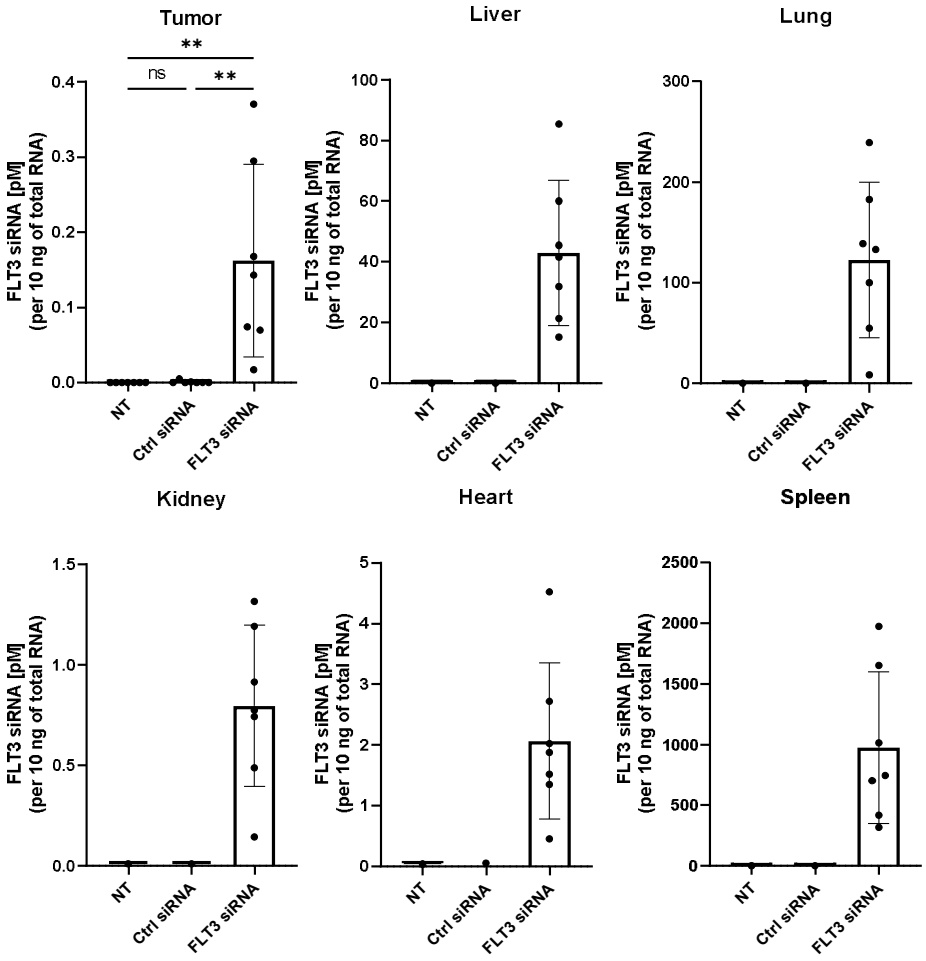

Figure 13. Biodistribution of siRNA in different organs in a xenograft AML model: Amount of FLT3 siRNA was determined in the tumor and other organs of mice injected with either vehicle, control siRNA or FLT3 siRNA, expressed as concentration of siRNA (pM) per 10 ng of total RNA. Organ collection was performed 72 hours after the last FLT3 siRNA injection. For tumors, all animals in all groups were analyzed. For the remaining organs, one single mouse was randomly selected from the untreated and control siRNA groups to validate qPCR specificity. Ordinary one-way ANOVA followed by a Tukey's multiple comparisons test, comparing all columns to each other (** p <0.01). NT: No treatment.

DISCUSSION

Pharmacotherapy involves the modification of the pathophysiology of a diseased cell or tissue, interfering with pathological processes and ultimately, aiming to bring back the tissue into normal

homeostasis. Therapeutic nucleic acids such as siRNAs are powerful tools that allow us to achieve the desired intervention for homeostasis by silencing the expression of harmful mRNAs into proteins, such as in the case of oncogenes and resultant neoplasms. Unfortunately, the physicochemical characteristics of nucleic acids such as their high charge density, large molecular size and low hydrophobicity, are not favourable for their biodistribution once injected into an animal model or a patient [28]. In this study, we explore how lipid-modified PEI-derived Leu-Fect carriers and the nanoparticles made with their complexation with siRNAs, can overcome some of these obstacles and become suitable delivery vehicles for siRNA for both *in vitro* and *in vivo* models of disease. We explored the delivery features in the context of hematological cancer leukemia, using CML and AML xenograft tumor models as paradigms.

The physical properties of the nanoparticles created with siRNA and the Leu-Fect carriers were first assessed. Regarding size, Leu-Fect A and C produced nanoparticles that were below the 200 nm mark, a size that is comparable to other successful delivery vehicles such as LNPs [29,30]. However, nanoparticles made with Leu-Fect B were almost double in size, perhaps posing a potential barrier to get the cargo across membranes, hindering biodistribution. This was in line with our observations in the animal model that Leu-Fect B formulated siRNA was in general poorly distributed when compared to nanoparticles made with the other two carriers. Although flocculation was not observed in the TEM analysis, the fact that Leu-Fect B nanoparticles had the lowest zeta potential and this perhaps facilitated the generation of few aggregates that may have skewed the results obtained in the zetasizer.

The binding affinity of carriers for siRNA is expected to play a crucial role when it comes to its delivery. It is known that polymers with higher affinities confer the cargo protection against serum degradation, but could also hinder the intracellular release of the cargo, reducing the silencing

efficacy [31,32]. Previous studies from our group have shown that distinct lipopolymers show adequate affinity for siRNAs since they have been successfully used for silencing a variety of target genes [16,18,19,33], but this is the first time we compare the physical properties of our distinct carriers head-to-head, finding that Leu-Fect A had the highest affinity based on binding and heparin dissociation analysis. We also demonstrated all three carriers conferred protection against serum degradation, a feature that is upmost required when attempting to deliver nucleic acids to cells in culture or in an animal model.

When siRNA was delivered to non-adherent cells such as leukemia cells, which are traditionally known to be more difficult to transfect [34,35], the polymeric Leu-Fect carriers were superior to lipofection in the case of siRNA delivery. Of the three carriers explored, Leu-Fect A was the best performer in MV4-11 under all conditions tested, and was the best performer in K562 cells at carrier/siRNA ratios up to 7.5:1. This was evidenced by flow cytometry and confocal microscopy experiments. It is likely that the high affinity for siRNA, and smaller size and higher ζ-potential of the resultant nanoparticles made Leu-Fect A display more favorable delivery capacity.

Although a carrier:siRNA ratio of 1:1 was enough to bind most of the siRNA in *in vitro* conditions where no other mayor negatively charged macromolecules were present, previous studies made with these carriers both *in vivo* and in cultured cells [16,27] have shown that efficacy is only observed at higher carrier:siRNA ratios. This may be explained by the presence of other negatively charged macromolecules present in the serum or blood that may compete for the binding sites at the carriers. Therefore, an excess of carrier may be needed to overcome this issue.

Needless to say, toxicity is a major consideration when a delivery vehicle is used as part of a therapy in animals and/or humans. In general, nanoparticles made with Leu-Fect carriers did not show toxicity when used at carrier/siRNA ratios up to 7.5:1, except for Leu-Fect C. The latter also

showed a higher hemolytic effect than their counterparts, suggesting that the toxic effect could be due to a direct interaction of the particle with the cellular membrane, rather than a specific biochemical event. This observation is supported in the fact that amongst the Leu-Fect carriers, Leu-Fect C generated complexes with the highest positive ζ-potential, a well-known risk factor for hemolysis [36]. It is interesting however that, when administered *in vivo* to mice, we did not observe an immediate or delayed effect on mouse health in any of our studies with the Leu-Fect carriers. We used a semi-quantitative scoring scale to assess the health of the mice on our study, as well as changes of mice weight among the study groups; there was no indication of undesirable effects in our studies. More subtle signs of toxicity were not evaluated in this study (e.g., hepatic ALT/AST levels in serum, bilirubin or LDH serum levels) and therefore more detailed studies will be needed in the future to unequivocally conclude on subtle toxicity, if any, of the carriers when used *in vivo.*

In terms of *in vivo* siRNA delivery performance, not all Leu-Fect carriers behaved the same and Leu-Fect A was undoubtably the best of the three carriers tested in our hands. This advantage could be the result of nanoparticles to be smaller in size with more positive ζ-potential and the carrier displaying a higher affinity for siRNA. It is also possible that the siRNA delivered with Leu-Fect A may have lasted inside the cells to a greater extent than other carriers (i.e., increased half-life intracellularly), facilitating its detection by the PCR techniques used in our study. However, the fact that we observed significant silencing of BCR-Abl mRNA in CML xenografts using Leu-Fect A confirmed the success of the siRNA delivery. It is also important to note that there seems to be a correlation between the siRNA binding affinity and efficacy of delivery, at least within the three Leu-Fect carriers assessed in the present study. While this study indicates effective delivery and availability of siRNA for target silencing, it is not known if all siRNA becomes available for

silencing or whether a fraction of the complexes remained intact, not providing the full siRNA dose. There was some evidence that not all bound siRNA was released from the complexes (especially with Leu-Fect A; see Fig 4), but whether a similar issue is valid under *in vivo* conditions remains to be seen. This will be the subject of future studies.

In all animal studies performed for this manuscript, we found that the Leu-Fect carriers preferentially delivered the siRNA into lungs, spleen and liver, being the delivery more widespread than what has been reported for other vehicles such as LNPs, where most of the therapeutic nucleic acid is delivered to the liver [37,38]. The carriers seem to preferentially deliver therapeutic nucleic acids to organs that are part of the reticuloendothelial system, a concern that has been explored in the past since it may reduce the delivery of nanoparticles to the desired target [39–41]. In addition, we also observed a better biodistribution of medicinal RNAs when using Leu-Fect A compared to LNPs, not only to the xenograft tumor, but also in the liver. Better protection of the encapsulated siRNA is the likely reason for this, given multivalent interactions between the polymeric Leu-Fect carrier and the siRNA that is bound to lead to better protection against the endogenous nucleases.

In conclusion, nanoparticles made with PEI-based Leu-Fect carriers are emerging as safe, reliable and effective vehicles for the delivery of medicinal nucleic acids, in this particular case, of siRNAs. In this pursuit, we found the molecular analysis tools such as stem-loop PCR followed by either qPCR or ddPCR are methods with high sensitivity and specificity, allowing us to accurately assess whether a medicinal nucleic acid has reached the target tissue. This may obviate the tracer methods based on radiolabeling and spectroscopic labels, which may alter the native physicochemical properties of the investigated ligand and lead to erroneous biodistribution information. The availability of reliable methods for the evaluation of biodistribution of siRNAs will certainly

accelerate the development of nanomedicines, not only for blood cancers, but for any disease where the silencing of a harmful gene may stop or delay the pathophysiological process.

DECLARATION OF INTERESTS

Luis C. Morales and Amarnath Rajendran are supported by RJH Biosciences Inc. via a MITACS Accelerate Grant. H. Uludag and Remant K.C. have ownership interest in RJH Biosciences Inc.

ACKNOWLEDGEMENTS

We gratefully acknowledge Marianna Kulka and Feng Wang of the Nanotechnology Research Centre (National Research Council of Canada, Edmonton, AB) for their assistance in LNP preparation. The study was supported by funding support from Canadian Institutes of Health Research (CIHR), Women and Children Health Research Institute (WCHRI) and Alex's Lemonade Stand Foundation (Innovation Grant) via operating funds. Equipment support was provided by Edmonton Civic Employees Charitable Assistance Fund (ECE-CAF).

REFERENCES

[1] A. Gupta, J.L. Andresen, R.S. Manan, R. Langer, Nucleic acid delivery for therapeutic applications, Adv. Drug Deliv. Rev. 178 (2021) 113834. https://doi.org/10.1016/j.addr.2021.113834.

[2] K. Heilbron, S.V. Mozaffari, V. Vacic, P. Yue, W. Wang, J. Shi, A.M. Jubb, S.J. Pitts, X. Wang, Advancing drug discovery using the power of the human genome, J. Pathol. 254 (2021) 418–429. https://doi.org/10.1002/path.5664.

[3] F.X. Heinz, K. Stiasny, Distinguishing features of current COVID-19 vaccines: knowns and unknowns of antigen presentation and modes of action, Npj Vaccines. 6 (2021) 104. https://doi.org/10.1038/s41541-021-00369-6.

[4] I. Urits, D. Swanson, M.C. Swett, A. Patel, K. Berardino, A. Amgalan, A.A. Berger, H. Kassem, A.D. Kaye, O. Viswanath, A Review of Patisiran (ONPATTRO®) for the Treatment of Polyneuropathy in People with Hereditary Transthyretin Amyloidosis, Neurol. Ther. 9 (2020) 301–315. https://doi.org/10.1007/s40120-020-00208-1.

[5] A.S. Desai, D.J. Webb, J. Taubel, S. Casey, Y. Cheng, G.J. Robbie, D. Foster, S.A. Huang, S. Rhyee, M.T. Sweetser, G.L. Bakris, Zilebesiran, an RNA Interference Therapeutic Agent for Hypertension, N. Engl. J. Med. 389 (2023) 228–238. https://doi.org/10.1056/NEJMoa2208391.

[6] B.B. Mendes, J. Conniot, A. Avital, D. Yao, X. Jiang, X. Zhou, N. Sharf-Pauker, Y. Xiao, O. Adir, H. Liang, J. Shi, A. Schroeder, J. Conde, Nanodelivery of nucleic acids, Nat. Rev. Methods Primer. 2 (2022) 24. https://doi.org/10.1038/s43586-022-00104-y.

[7] R. Selot, S. Hareendran, G. Jayandharan, Developing Immunologically Inert Adeno-Associated Virus (AAV) Vectors for Gene Therapy: Possibilities and Limitations, Curr. Pharm. Biotechnol. 14 (2014) 1072–1082. https://doi.org/10.2174/1389201015666140327141710.

[8] J.T. Bulcha, Y. Wang, H. Ma, P.W.L. Tai, G. Gao, Viral vector platforms within the gene therapy landscape, Signal Transduct. Target. Ther. 6 (2021) 53. https://doi.org/10.1038/s41392-021-00487-6.

[9] H. Zu, D. Gao, Non-viral Vectors in Gene Therapy: Recent Development, Challenges, and Prospects, AAPS J. 23 (2021) 78. https://doi.org/10.1208/s12248-021-00608-7.

[10] H. Wang, X. Liu, X. Ai, K.C. Remant-Bahadur, T.A. Dick, B. Yan, T. Lu, X. Zhou, R. Luo, M. Liu, X. Wang, K. Li, W. Wang, H. Uludag, W. Fu, Safe and Effective Delivery of mRNA Using Modified PEI-Based Lipopolymers, Pharmaceutics. 15 (2023) 410. https://doi.org/10.3390/pharmaceutics15020410.

[11] H. Yin, R.L. Kanasty, A.A. Eltoukhy, A.J. Vegas, J.R. Dorkin, D.G. Anderson, Non-viral vectors for gene-based therapy, Nat. Rev. Genet. 15 (2014) 541–555. https://doi.org/10.1038/nrg3763.

[12] Z. Chen, Z. Lv, Y. Sun, Z. Chi, G. Qing, Recent advancements in polyethyleneimine-based materials and their biomedical, biotechnology, and biomaterial applications, J. Mater. Chem. B. 8 (2020) 2951–2973. https://doi.org/10.1039/C9TB02271F.

[13] J. Proulx, C. Joshi, S. Vijayaraghavalu, M. Saraswathy, V. Labhasetwar, A. Ghorpade, K. Borgmann, Arginine-Modified Polymers Facilitate Poly (Lactide-Co-Glycolide)-Based Nanoparticle Gene Delivery to Primary Human Astrocytes, Int. J. Nanomedicine. Volume 15 (2020) 3639–3647. https://doi.org/10.2147/IJN.S250865.

[14] S. Lu, X. Bao, W. Hai, S. Shi, Y. Chen, Q. Yu, M. Zhang, Y. Xu, J. Peng, Multi-functional self-assembled nanoparticles for pVEGF-shRNA loading and anti-tumor targeted therapy, Int. J. Pharm. 575 (2020) 118898. https://doi.org/10.1016/j.ijpharm.2019.118898.
[15] A.P. Rajendran, O. Ogundana, L.C. Morales, D.N. Meenakshi Sundaram, C. Kucharski, R. Kc, H. Uludağ, Transfection Efficacy and Cellular Uptake of Lipid-Modified Polyethyleneimine Derivatives for Anionic Nanoparticles as Gene Delivery Vectors, ACS Appl. Bio Mater. 6 (2023) 1105–1121. https://doi.org/10.1021/acsabm.2c00978.
[16] T. Santadkha, W. Skolpap, R. K C, A. Ansari, C. Kucharski, T. Atz Dick, H. Uludağ, Improved delivery of Mcl-1 and survivin siRNA combination in breast cancer cells with additive siRNA complexes, Invest. New Drugs. 40 (2022) 962–976. https://doi.org/10.1007/s10637-022-01282-y.
[17] D.N. Meenakshi Sundaram, S. Plianwong, R. Kc, H. Ostergaard, H. Uludağ, In Vitro Cytotoxicity and Cytokine Production by Lipid-Substituted Low Molecular Weight Branched PEIs Used for Gene Delivery, Acta Biomater. 148 (2022) 279–297. https://doi.org/10.1016/j.actbio.2022.06.030.
[18] D.N. Meenakshi Sundaram, R.B. Kc, H. Uludağ, Linoleic-acid-substituted polyethylenimine to silence heat shock protein 90B1 (HSP90B1) to inhibit migration of breast cancer cells, J. Gene Med. 24 (2022) e3419. https://doi.org/10.1002/jgm.3419.
[19] K.C. Remant, B. Thapa, J. Valencia-Serna, S.S. Domun, C. Dimitroff, X. Jiang, H. Uludağ, Cholesterol grafted cationic lipopolymers: Potential siRNA carriers for selective chronic myeloid leukemia therapy, J. Biomed. Mater. Res. A. 108 (2020) 565–580. https://doi.org/10.1002/jbm.a.36837.
[20] J. Valencia-Serna, C. Kucharski, M. Chen, R. Kc, X. Jiang, J. Brandwein, H. Uludağ, siRNA-mediated BCR-ABL silencing in primary chronic myeloid leukemia cells using lipopolymers, J. Control. Release Off. J. Control. Release Soc. 310 (2019) 141–154. https://doi.org/10.1016/j.jconrel.2019.08.018.
[21] S. Plianwong, B. Thapa, R.B. Kc, C. Kucharski, T. Rojanarata, H. Uludağ, Enabling Combinatorial siRNA Delivery against Apoptosis-Related Proteins with Linoleic Acid and α-Linoleic Acid Substituted Low Molecular Weight Polyethylenimines, Pharm. Res. 37 (2020) 46. https://doi.org/10.1007/s11095-020-2770-9.
[22] A.K.K. Leung, Y.Y.C. Tam, S. Chen, I.M. Hafez, P.R. Cullis, Microfluidic Mixing: A General Method for Encapsulating Macromolecules in Lipid Nanoparticle Systems, J. Phys. Chem. B. 119 (2015) 8698–8706. https://doi.org/10.1021/acs.jpcb.5b02891.
[23] K.K. Son, D. Tkach, D.H. Patel, Zeta potential of transfection complexes formed in serum-free medium can predict in vitro gene transfer efficiency of transfection reagent, Biochim. Biophys. Acta BBA - Biomembr. 1468 (2000) 11–14. https://doi.org/10.1016/S0005-2736(00)00312-6.
[24] Y. Hattori, M. Hashida, Evaluation of Size and Zeta Potential of DNA/Carrier Complexes, in: K. Taira, K. Kataoka, T. Niidome (Eds.), Non-Viral Gene Ther., Springer-Verlag, Tokyo, 2005: pp. 293–299. https://doi.org/10.1007/4-431-27879-6_22.
[25] K.C. Remant Bahadur, B. Landry, H.M. Aliabadi, A. Lavasanifar, H. Uludağ, Lipid substitution on low molecular weight (0.6–2.0 kDa) polyethylenimine leads to a higher zeta potential of plasmid DNA and enhances transgene expression, Acta Biomater. 7 (2011) 2209–2217. https://doi.org/10.1016/j.actbio.2011.01.027.

[26] L. Xu, X. Wang, Y. Liu, G. Yang, R.J. Falconer, C.-X. Zhao, Lipid Nanoparticles for Drug Delivery, Adv. NanoBiomed Res. 2 (2022) 2100109. https://doi.org/10.1002/anbr.202100109.
[27] J. Valencia-Serna, H.M. Aliabadi, A. Manfrin, M. Mohseni, X. Jiang, H. Uludag, siRNA/lipopolymer nanoparticles to arrest growth of chronic myeloid leukemia cells in vitro and in vivo, Eur. J. Pharm. Biopharm. 130 (2018) 66–70. https://doi.org/10.1016/j.ejpb.2018.06.018.
[28] J.A. Kulkarni, D. Witzigmann, S.B. Thomson, S. Chen, B.R. Leavitt, P.R. Cullis, R. Van Der Meel, The current landscape of nucleic acid therapeutics, Nat. Nanotechnol. 16 (2021) 630–643. https://doi.org/10.1038/s41565-021-00898-0.
[29] S. Barua, S. Mitragotri, Challenges associated with penetration of nanoparticles across cell and tissue barriers: A review of current status and future prospects, Nano Today. 9 (2014) 223–243. https://doi.org/10.1016/j.nantod.2014.04.008.
[30] Y. Eygeris, M. Gupta, J. Kim, G. Sahay, Chemistry of Lipid Nanoparticles for RNA Delivery, Acc. Chem. Res. 55 (2022) 2–12. https://doi.org/10.1021/acs.accounts.1c00544.
[31] L. Han, C. Tang, C. Yin, Effect of binding affinity for siRNA on the in vivo antitumor efficacy of polyplexes, Biomaterials. 34 (2013) 5317–5327. https://doi.org/10.1016/j.biomaterials.2013.03.060.
[32] H. Wang, S. Zhang, J. Lv, Y. Cheng, Design of polymers for siRNA delivery: Recent progress and challenges, VIEW. 2 (2021) 20200026. https://doi.org/10.1002/VIW.20200026.
[33] M. Mohseni, C. Kucharski, R.B. K C, M. Nasrullah, X. Jiang, H. Uludağ, J. Brandwein, Therapeutic delivery of siRNA with polymeric carriers to down-regulate STAT5A expression in high-risk B-cell acute lymphoblastic leukemia (B-ALL), PloS One. 16 (2021) e0251719. https://doi.org/10.1371/journal.pone.0251719.
[34] Z.X. Chong, S.K. Yeap, W.Y. Ho, Transfection types, methods and strategies: a technical review, PeerJ. 9 (2021) e11165. https://doi.org/10.7717/peerj.11165.
[35] S. Basiouni, H. Fuhrmann, J. Schumann, High-efficiency transfection of suspension cell lines, BioTechniques. 53 (2012) 1–4. https://doi.org/10.2144/000113914.
[36] W.-S. Cho, F. Thielbeer, R. Duffin, E.M.V. Johansson, I.L. Megson, W. MacNee, M. Bradley, K. Donaldson, Surface functionalization affects the zeta potential, coronal stability and membranolytic activity of polymeric nanoparticles, Nanotoxicology. 8 (2014) 202–211. https://doi.org/10.3109/17435390.2013.773465.
[37] B. Shi, E. Keough, A. Matter, K. Leander, S. Young, E. Carlini, A.B. Sachs, W. Tao, M. Abrams, B. Howell, L. Sepp-Lorenzino, Biodistribution of Small Interfering RNA at the Organ and Cellular Levels after Lipid Nanoparticle-mediated Delivery, J. Histochem. Cytochem. 59 (2011) 727–740. https://doi.org/10.1369/0022155411410885.
[38] C.D. Sago, B.R. Krupczak, M.P. Lokugamage, Z. Gan, J.E. Dahlman, Cell Subtypes Within the Liver Microenvironment Differentially Interact with Lipid Nanoparticles, Cell. Mol. Bioeng. 12 (2019) 389–397. https://doi.org/10.1007/s12195-019-00573-4.
[39] S. Nie, Understanding and overcoming major barriers in cancer nanomedicine, Nanomed. 5 (2010) 523–528. https://doi.org/10.2217/nnm.10.23.
[40] Y. Tang, X. Wang, J. Li, Y. Nie, G. Liao, Y. Yu, C. Li, Overcoming the Reticuloendothelial System Barrier to Drug Delivery with a “Don’t-Eat-Us” Strategy, ACS Nano. 13 (2019) 13015–13026. https://doi.org/10.1021/acsnano.9b05679.
[41] I.B. Magaña, R.B. Yendluri, P. Adhikari, G.P. Goodrich, J.A. Schwartz, E.A. Sherer, D.P. O’Neal, Suppression of the reticuloendothelial system using λ-carrageenan to prolong

the circulation of gold nanoparticles, Ther. Deliv. 6 (2015) 777–783. https://doi.org/10.4155/tde.15.33.